JOURNAL OF CATALYSIS 140, 564–574 (1993)

CO-Induced Changes in the Oxidation State of Rhodium Supported on MgO: X-Ray Photoelectron Spectroscopic Study

ANGELOS M. EFSTATHIOU,*,[1] BENG JIT TAN,*,† AND STEVEN L. SUIB*,†,‡,[2]

*Department of Chemical Engineering, †Institute of Materials Science, and ‡Department of Chemistry, U-60, University of Connecticut, Storrs, Connecticut 06269

Received July 16, 1992; revised October 29, 1992

The oxidation state of Rh after various CO/He treatments with a 2.5 wt% Rh/MgO catalyst was investigated with X-ray photoelectron spectroscopy. The rhodium metal particles, initially in a reduced state (Rh^0), were found to be partially oxidized (Rh^{n+}) after treatment with CO/He at $T < 523$ K followed by heating in He to 723 K. The formation of Rh^{n+} species depends on H_2 reduction conditions applied before the exposure of the catalyst to CO/He. The amount of Rh^{n+} species formed decreases with increasing H_2 reduction temperature. © 1993 Academic Press, Inc.

INTRODUCTION

The chemistry of interaction between CO and Rh-supported catalysts has recently captured the attention of many researchers. EXAFS work of Prins and co-workers (*1*) on a 0.5-wt% Rh/Al_2O_3 catalyst has shown that CO can cause disruption of small Rh crystallites and the formation of isolated Rh^+ sites. More recently many other workers have used infrared spectroscopy to show that CO adsorption can cause the disruption of small and large Rh crystallites supported on Al_2O_3, SiO_2, and TiO_2 (*2–6*). Basu *et al.* (*5*) first demonstrated the direct correlation of specific-OH groups of the oxide support to the formation of $Rh^I(CO)_2$ species in the presence of gaseous CO. Structural degradation phenomena of Rh crystallites induced by CO and affected by (a) preadsorbed H_2 (*7*), (b) temperature of CO chemisorption (*4, 6*), (c) presence of H_2O (*4*), and (d) promoters (*3, 8*) have also been studied.

The objective of the present work was to study the effects of various CO/He treatments with the Rh/MgO catalyst on the oxidation state of Rh. The effects of H_2 reduction temperature, following CO/He treatment, on the Rh oxidation state were also studied. In the present work, X-ray photoelectron spectroscopy was used exclusively. XPS has proved to be an extremely useful technique in the determination of chemical states of supported metal catalysts and metal films (*9–13*). The results obtained are discussed in relation to others obtained by infrared and temperature-programmed desorption (TPD) spectroscopies on the same catalyst (*14, 15*). To our knowledge, the oxidation state of Rh supported on MgO as obtained after CO/He treatments in the range 300–573 K has not been previously studied.

EXPERIMENTAL

Catalyst. A 2.5-wt% Rh/MgO catalyst was prepared by impregnating MgO (99.9% AESAR Co.) to incipient wetness (1.4 mL/g MgO) with an ethanol solution of $RhCl_3 \cdot 3H_2O$ (Aldrich Co.). The MgO was first treated at 773 K for 24 h in a Pt crucible in an air environment. The impregnated catalyst was dried at 300 K for 40 h and then at 393 K for 4 h, pressed at 130 bar to form a disk of about 0.25 mm thickness, crushed, and then screened to give 0.58-mm particles.

[1] Present address: Institute of Chemical Engineering and High Temperature Chemical Processes, GR-26110, Patras, Greece.

[2] To whom correspondence should be addressed.

0021-9517/93 $5.00

Samples were passivated by treating them in hydrogen at 573 K for 2 h, then calcining them in oxygen at 673 K for 2 h. Details of the preparation were reported (*16*). The BET surface area of the support (30 m^2/g), the active metal surface (3.58 m^2/g), and the fraction exposed, FE (0.31), of the fresh samples were measured as described elsewhere (*14, 16*).

XPS measurements. X-ray photoelectron spectroscopy measurements were carried out using a Leybold Heraeus EA10 system and Mg$K\alpha$ X-ray radiation. The power was 130 W (13 keV, 10 mA). The base pressure in the sample chamber was 3×10^{-9} Torr. Low-resolution broad scans were collected at a fixed retardation ratio of 3 (FRR 3) in order to survey elemental composition over the entire XPS energy range. High-resolution spectra were collected at a pass energy of 50 eV fixed analyzer transmission (FAT 50) to obtain more detailed chemical information of the catalyst surface. At this pass energy, the peak width for the Ag $3d_{5/2}$ line is 0.7 eV. The sample spot size is 2 mm × 10 mm. Calibration was based upon the C 1*s* photoelectron peak of adventitious carbon at 284.6 eV. No detrimental effects of exposure to the X-ray beam were observed. Peak areas were calculated through a normalization which accounted for acquisition time and step size of data points. No charge neutralization was used; samples were exposed to the incident X-ray beam for at least 10 min to allow the sample to acquire charge equilibration before acquiring spectra. By this time no differential charging of the sample was observed and similar charging shifts were noted for the C 1*s* and Rh 3*d* lines. Satellite lines were subtracted by computer software curve-fitting analyses. XPS spectra are fitted to a Gaussian/Lorentzian function with a mixing ratio of 0.5 for all peaks. The tail parameters are different for the oxide and metal peaks. An exponential tail characteristic to the high-binding-energy side of the metal peaks is added to the lineshape of metal peaks to account for the asymmetry in the metal peak shape due to conduction band interaction effects (*17–20*). A nonlinear background was adapted to account for inelastic electron ejection processes (*21, 22*).

Reactor-flow system. A stainless steel reactor of 15 ml volume was used in this study. The reactor was directly connected to the XPS instrument so that the catalyst could be brought into the XPS spectrometer for spectral collection after various gas reactions without air contact. The preparation of the 9.9-mol% CO/He mixture has been described (*16*). The He gas was zero grade (Aero All-Gas Co.), and the H_2 was standard grade (99.98%). Helium was also used as a purging gas. All gases were used at a flow rate of 30 ml/min (ambient) and 1 bar total pressure.

Sample treatments. All gas treatments of the catalyst sample and XPS measurements were carried out on a single sample unless otherwise stated. The sample gas treatments are summarized in Table 1. These were carried out in successive order. Spectra were acquired at the end of each sample gas treatment. The reaction chamber was backfilled with either He or H_2 before the start of each gas treatment.

RESULTS

(*A*) *Effects of Reaction Temperature in CO/He*

Of interest in the present work are the Rh 3d, O 1s, C 1s and Mg 2s core-level XPS peaks. Figures 1–3 show Rh 3*d* XPS spectra of the Rh/MgO catalyst for the various treatments given in Table 1. The peak positions and other peak parameters of the Rh 3*d* region are summarized in Table 2. For Fig. 1 (fresh calcined sample), the Rh $3d_{5/2}$ and Rh $3d_{3/2}$ peaks are found at binding energies of 315.5 and 310.7 eV, respectively, corresponding to those of Rh_2O_3 (*23*). Hydrogen reduction at 623 K (Fig. 2a) results in complete reduction of the Rh_2O_3 to Rh metal accompanied by a shift in the Rh 3*d* doublet towards lower binding energies (311.9 and 307.2 eV) (*24*) from those of the fresh calcined sample. The doublet peaks were curve

TABLE 1

Treatments of Rh/MgO Catalyst Samples

Treatment[a]	Treatment description
a	Fresh calcined catalyst.
b	Reduced in hydrogen at 623 K for 2 h. Cooled in hydrogen to r.t.[b]
c	Reduced in hydrogen at 623 K, cooled in H_2 to r.t. CO/He at r.t. for 30 min. Heated in He to 723 K, held at 723 K for 5 min. Cooled to r.t. in He.
d	Reduced in hydrogen at 623 K, CO/He at 423 K for 30 min. Cooled in CO/He. Heated to 723 K in He. Cooled to r.t. in He.
e	Reduced in H_2 at 623 K, cooled to r.t. in H_2. Treated with CO/He at 523 K, held at 523 K in CO/He. Cooled to r.t. in CO/He.
f	Reduced in H_2 at 623 K. Cooled to r.t. in H_2. Treated in CO/He at 573 K for 60 min. Cooled in CO/He to r.t.
g	Reduced in H_2 at 623 K, cooled to r.t. in H_2. Reduced in hydrogen at 623 K for 30 min. Cooled in hydrogen at r.t. Treated in CO/He at 573 K for 60 min. Cooled in CO/He to r.t. Heated in He to 723 K. Cooled to r.t. in He.
h	Reduced in hydrogen at 623 K. Treated in CO/He at 723 K for 30 min. Cooled to r.t. in CO/He.
i	Reduced in H_2 at 623 K. Heated to 723 K in He. Held at 723 K in He for 5 min. Cooled to r.t. in He.
j	Reduced in hydrogen at 623 K for 2 h. CO/He at 573 K for 5 min. Cooled to r.t. in He.
k	Reduced in hydrogen at 773 K. CO/He at r.t. for 30 min, heated to 723 K in He, held at 723 K for 5 min. Cooled to r.t. in He.

[a] Treatments a through i were done on one sample. Treatments j and k were each done on a new fresh catalyst sample.

[b] r.t. = room temperature.

fitted with an exponential tail due to the metallic character of the reduced sample. The full-width at half maximum (FWHM) for the Rh $3d_{3/2}$ peak decreased from 3.3 to 2.3 eV in going from the oxidized to the reduced state.

On exposure of the reduced sample (H_2 at 623 K) to the CO/He mixture at 300 K, followed by the treatments described in Table 1, four peaks are observed (Fig. 2b) which can be ascribed to two sets of Rh 3*d* peaks arising from two different oxidation states of rhodium. The peaks at 314.5 and 309.9 eV correspond to an oxidized state, and the peaks at 311.8 and 307.2 eV to a fully reduced metallic state.

Similar treatments with CO/He at 423 and 523 K also result in an oxidized Rh^{n+} state in addition to metallic Rh^0 (Figs. 2c and 2d, respectively). However, the oxidized Rh^{n+} state is absent when the Rh/MgO catalyst is treated with CO/He at temperatures above 573 K (Figs. 3a–3c). Treatment of freshly reduced catalyst with helium alone at 723 K did not result in the formation of oxidized rhodium species (Fig. 3d). When CO/He reaction was carried out at 573 K on another fresh calcined sample (after being reduced with H_2 at 623 K), no oxidized Rh species were observed (Fig. 4a) and only a doublet corresponding to the fully reduced Rh^0 state was obtained (Table 2).

The peak parameters and area ratios of the O 1*s* peak are summarized in Table 3. The O 1*s* spectrum of the fresh calcined sample, as well as those after CO/He treatments, are curve-fitted to two peaks with binding energies of 532.4 and 530.5 eV. Peak 1 at 532.4 ± 0.2 eV is attributed to surface hydroxyl groups (*25*), while Peak 2 at 530.5 ± 0.2 eV to MgO (*26*) and Rh_2O_3 (*23*). The O 1*s* peaks of MgO and Rh_2O_3 cannot be distinguished at the resolution of our XPS instrument. Hydrogen reduction at 623 K

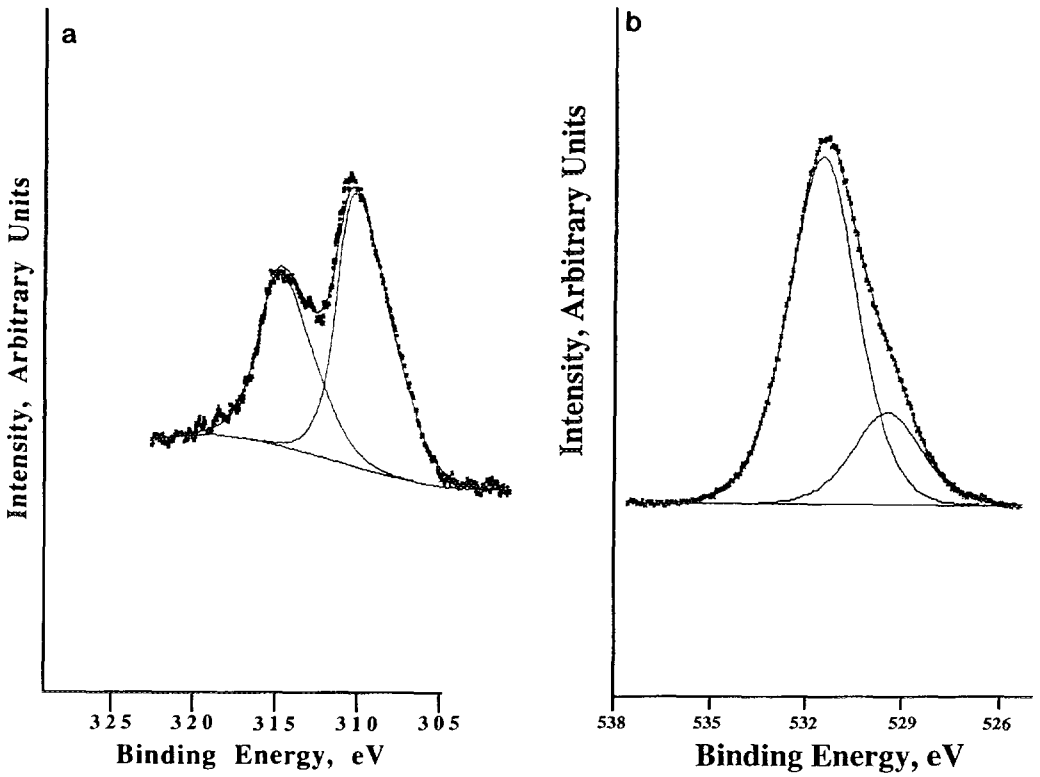

FIG. 1. (a) Rh 3*d* and (b) O 1*s* core-level photoelectron spectra of fresh calcined Rh/MgO catalysts (treatment a).

readily removes the adsorbed H_2O from the surface and reduces the Rh_2O_3 to Rh (Fig. 2a). This results in a decrease of the peak area ratio of the surface hydroxyl species to the metal oxide (MgO and Rh_2O_3) from 3.74 to 0.18. The results of Table 3 show that further CO/He treatments of the sample do not alter this peak intensity ratio.

Atomic concentration ratios for the various gas treatments described in Table 1 are given in Table 4. The Rh/Mg atomic ratio for the reduced sample (Fig. 2a) is 0.06. This ratio increases to 0.08–0.10 when the sample was exposed to CO/He at adsorption temperatures no higher than 523 K (Figs. 2b–2d). The ratio decreased to 0.03 when the CO/He adsorption temperature was raised above 523 K (Figs. 3a–3c). Exposing the reduced sample to He alone at 723 K (Fig. 3d) caused the Rh/Mg atomic ratio to increase to 0.06, similar to that of the freshly reduced sample (Fig. 2).

There is an increase in the Rh/O atomic ratio, from 0.07 to 0.08 after CO/He treatments at $T < 523$ K with respect to the freshly reduced sample. CO/He treatments at $T > 523$ K caused a decrease in the Rh/O atomic ratio to a value of 0.03.

(*B*) *Effects of H_2 Reduction Temperature*

When a freshly calcined Rh/MgO sample was subjected to a H_2 reduction treatment at 773 K followed by a CO/He treatment at 300 K, only a small amount of Rh^{n+} species was obtained (Fig. 4b). The predominant species was metallic Rh (compare Table 5,c and k).

This observation is supported by a further increase in the Rh/O atomic ratio (compare Table 4,c and k) accompanied by a slight

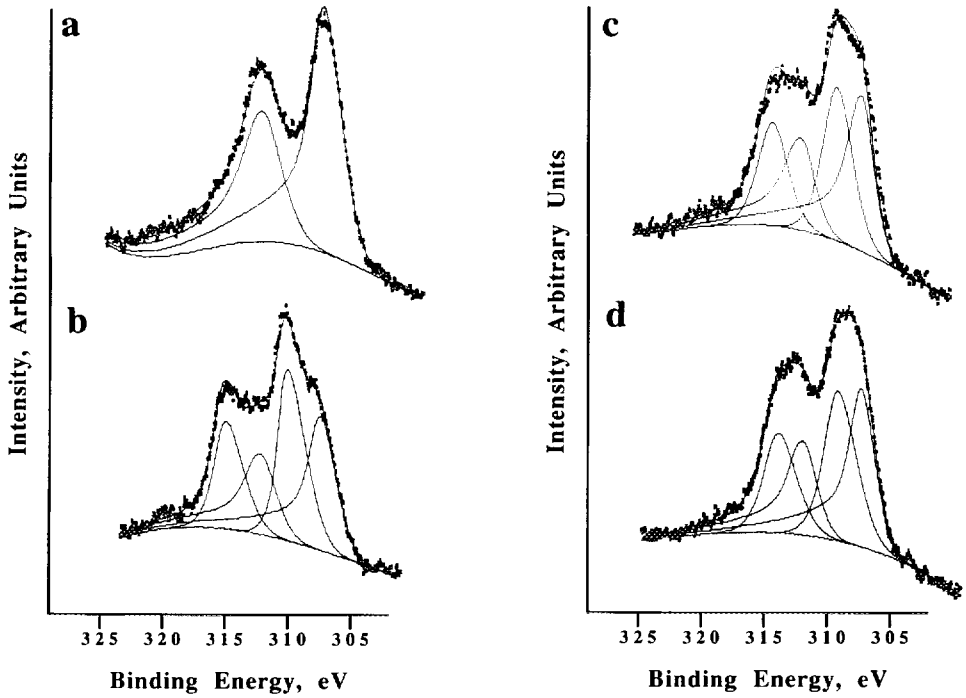

FIG. 2. Rh 3*d* photoelectron spectrum of catalyst: (a) reduced in hydrogen at 623 K and cooled to room temperature (r.t.) in hydrogen (treatment b); (b) reduction in hydrogen at 623 K, cooled to r.t. in hydrogen, followed by CO/He adsorption at r.t. for 30 min., heated to 723 K in He, and then cooled to r.t. in He (treatment c); (c) reduced in hydrogen at 623 K, cooled to r.t. in hydrogen, followed by CO/He adsorption at 423 K for 30 min., heated to 723 K in He, and then cooled to r.t. in He (treatment d); (d) reduced in hydrogen at 623 K, cooled to r.t. in hydrogen, followed by CO/He adsorption at 523 K for 30 min., heated to 723 K in He, and then cooled to r.t. in He (treatment e).

decrease in the ratio of the O 1*s* peak component peak area (compare Table 3,c and k). It is noted, however, that reduction at the higher temperature followed by CO/He treatment results in a lower Rh/Mg atomic ratio (compare Table 4,e and k).

DISCUSSION

(*A*) *Effects of CO/He Treatment at 300 K Followed by Heating in He to 723 K*

The oxidation state of Rh before its first exposure to the CO/He mixture is that of Rh^0 (Fig. 2a). The 3.5-eV downward shift in binding energy positions of the Rh 3*d* peak indicates complete reduction of Rh^{3+} at 623 K. This agrees with the results of Buchanan *et al.* (*6*) on a Rh/TiO_2 catalyst. Adsorption of CO at 300 K on a reduced Rh surface, precovered with a monolayer of hydrogen, followed by a He purge to 723 K produced two sets of doublets in the Rh 3d region (Fig. 2b). The doublet at the lower binding energy, (311.9, 307.2 eV) corresponds to metallic Rh^0 (*23*), while that at higher energy (314.5, 309.9 eV) suggests an oxidized Rh state (Rh^{n+}). It is not possible to assign unambiguously the oxidation state of the Rh^{n+} species. The peak position of the Rh $3d_{5/2}$ peak at 309.9 eV is too high in binding energy to be assigned to Rh^+ which has a binding energy of 308.0 eV (*27*). The binding energy of 309.9 eV falls in between the reported binding energies of Rh^{2+} (309.1 eV) (*23*d) and Rh^{3+} (310.7 eV) (*23*). Future EPR work may be able to help in the assign-

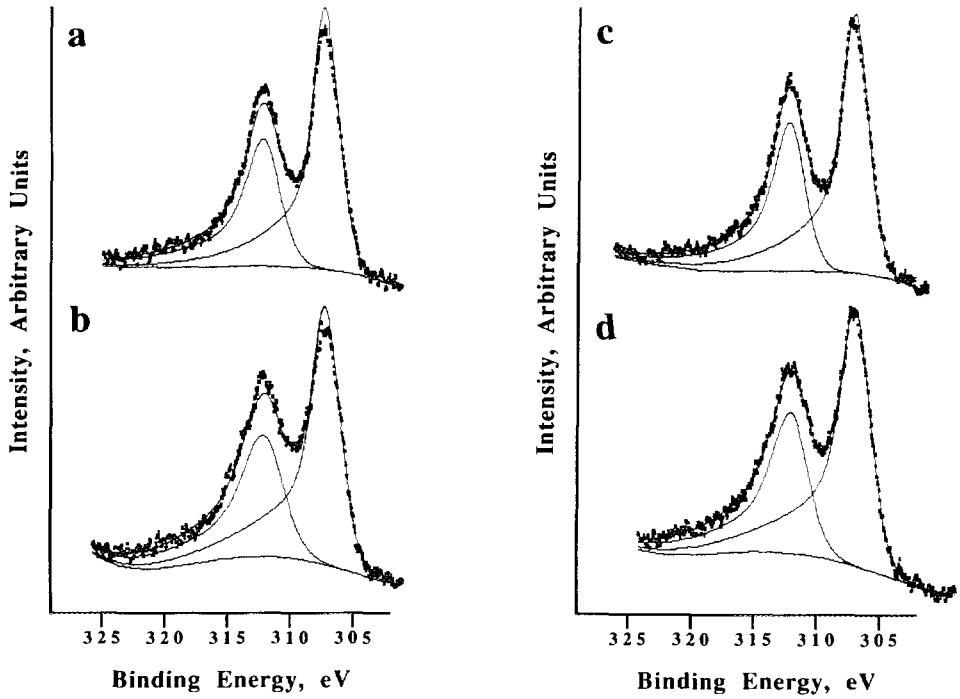

FIG. 3. Rh 3*d* photoelectron spectrum of catalyst: (a) reduced in hydrogen at 623 K, cooled to r.t. in hydrogen, followed by CO/He adsorption at 573 K for 60 min. The sample was then cooled to r.t. in CO/He (treatment f); (b) reduced in hydrogen at 623 K, cooled to r.t. in hydrogen, followed by CO/He adsorption at 573 K for 60 min. The sample was then cooled to r.t. in CO/He, heated to 723 K in He, and then recooled to r.t. in He (treatment g); (c) reduced in hydrogen at 623 K, cooled to r.t. in hydrogen, followed by CO/He adsorption at 723 K for 30 min. The sample was then recooled to r.t. in CO/He (treatment h); (d) reduced in hydrogen at 623 K and cooled to r.t. in hydrogen. The sample was then heated to 723 K in He and recooled to r.t. in He (treatment i).

ment of the oxidation state to the Rh^{n+} species.

In recent XPS work on a Rh/TiO_2 catalyst, Buchanan *et al.* (*6*) have observed the formation of oxidized Rh species after treatment with CO at 300 K. Their work is different from the present one in two aspects excluding potential support effects. First, in their experiments, the Rh surface, before CO chemisorption, did not contain any adsorbed hydrogen (opposite to the present case), and second, no He purge to 723 K, following chemisorption of CO, was applied (opposite to the present case). However, their XPS Rh 3*d* spectrum is similar to the one observed here (Fig. 2b) corresponding to a mixture of Rh oxidation states.

The results of Figs. 1, 2a–2b, and Table 2,a–c, unambiguously indicate that adsorption of CO on a reduced Rh/MgO catalyst induced oxidation of the Rh surface. Adsorbed hydrogen did not prevent this oxidation. Many previous reports presented evidence that adsorption of CO at 300 K can cause the disruption of Rh_x^0 crystallites into smaller ones and/or isolated Rh^0 atoms (*1–6*). Oxidation of Rh^0 then occurs with the aid of $-OH$ groups of the support as shown in Scheme I and represented in Eq. (1),

$$Rh^0 + OH^- \leftrightarrow Rh^+ + \tfrac{1}{2} H_2 + O^{2-}, \quad (1)$$

where the nature of OH^- groups is important for this reaction (*5, 6*). Development

TABLE 2

Peak Positions[a], Areas, and Widths[b] of the Rh 3*d* Region of the Rh/MgO Catalyst after Various CO/He Adsorption Treatments

Treatment	Rh $3d_{3/2}$			Rh $3d_{5/2}$		
	B.E. (eV)	Area	FWHM (eV)	B.E. (eV)	Area	FWHM (eV)
a	310.7	71566	3.3	315.5	47734	3.8
b	307.2	191534	2.3	311.9	127833	2.9
c	307.2	80534	2	311.8	53716	2.2
	309.9	72132	2.3	314.5	48112	2.5
d	307.2	77228	2	311.8	51511	2.3
	309.8	58952	2.3	314.5	39321	2.5
e	307.2	102020	2	311.8	68048	2.2
	309.8	86891	2.4	314.5	57956	2.6
f	307.2	155123	2	311.7	103467	2.5
g	307.2	148258	2.2	311.8	98888	2.6
h	307.1	147700	2	311.8	98516	2.3
i	307.1	159998	2.1	311.8	106719	2.5
j	307.2	157770	2.1	311.9	105233	2.6
k	307.2	72446	2	311.8	48321	2.2
	309.8	47987	2.3	314.5	3199	2.5

[a] Binding energy (B.E.) in eV referenced to C 1*s* = 284.6 eV.
[b] Full-width at half maximum (FWHM) in eV.

of gem-dicarbonyl species upon adsorption of CO at 300 K is believed to be associated with Rh^+ sites (*1–6*). In the present work, we did observe oxidation of the Rh surface by CO adsorption at 300 K (Fig. 2b) consistent also with infrared results (development of gem-dicarbonyl CO species) obtained with the present catalyst (*15*). Note that desorption of CO in the range 300–723 K (before the XPS measurements) did not cause reduction of the oxidized Rh surface.

Other sources of oxygen were considered, namely, oxygen impurities in the He carrier gas and oxygen species derived from the dissociation of CO. The possibility that the result of Fig. 2b is due to oxidation of Rh^0 by oxygen species derived from the dissociation of CO above 473 K (*9*), during He treatment to 723 K, is excluded. If this were the case, then one should also expect oxidation of Rh in the cases where more oxygen species are expected to be found on the Rh surface (Figs. 3a–3c). In addition, the results of Fig. 3d exclude the possibility of

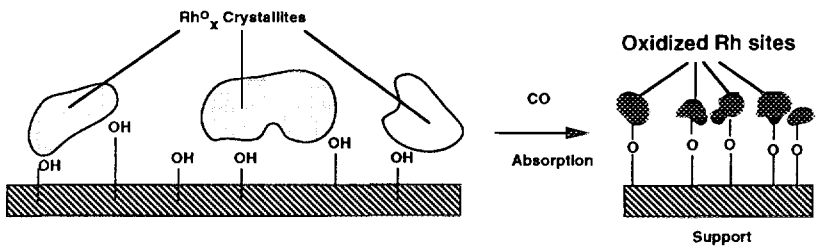

SCHEME 1. Oxidation disruption effect of CO absorption. CO/He treatments at temperatures lower than 573 K.

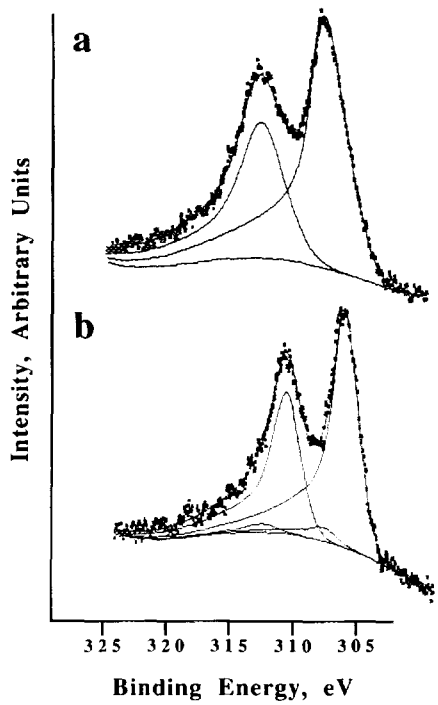

FIG. 4. Rh 3*d* spectrum of catalyst: (a) reduced in hydrogen at 623 K, CO/He adsorption at 573 K for 5 min, and recooled to r.t. in He (treatment j); (b) reduced in hydrogen at 773 K, cooled to r.t. in hydrogen, followed by CO/He adsorption at r.t. for 30 min. The sample was reheated to 723 K in He and then cooled to r.t. in He (treatment k).

oxygen impurities in the He carrier gas being the cause of oxidation of the Rh surface. Indeed, the atomic ratios and peak area ratios calculated for treatments b and i (Tables 3–5) are identical. The agreement in these ratios between treatments b and i lends strong support that the changes observed in Rh/MgO catalysts in the present study are due to the effect of CO and not the carrier gas.

The results of Fig. 2b and Table 5 indicate that a substantial amount of metallic Rh^0 is present after the CO/He treatment at 300 K followed by He TPD to 723 K. This result is consistent with infrared work on the present catalyst (*15*), where linear and bridge-type CO species associated with Rh_x^0 were found.

(*B*) *Effects of CO/He Treatment in the Range 423–723 K Followed by Heating in He to 723 K*

Table 5 indicates that the extent of oxidation of the Rh surface is about the same for CO/He treatments done at 423 or 523 K. Infrared work on the present catalyst (*15*) indicated a small amount of gem-dicarbonyl CO after adsorption at these temperatures. In addition, heating the sample in He following adsorption of CO at 300 K, caused the desorption of gem-dicarbonyl CO groups before 523 K. These results suggest that the extent of the oxidative disruptive effect of CO on the Rh_x^0 crystallites in the range 423–523 K is similar to that at 300 K, and at these temperatures the CO does not induce the reductive agglomeration of oxidized Rh sites to Rh_x^0. The latter was also

TABLE 3

Peak Positions,[a] Areas,[b] and FWHM[c] for the O 1*s* Region of Rh/MgO Catalyst after Various CO/He Treatments

Treatment[d]	Peak 1	Peak 2	FWHM	Peak 1/Peak 2 area ratio
a	532.3	530.3	2.2	
	[7321]	[1956]		3.74
b	532.2	530.2	2.1	
	[7328]	[40,712]		0.18
c	532.4	430.2	2.2	
	[19,442]	[114,141]		0.17
d	532.3	530.2	2.2	
	[11,439]	[67,209]		0.17
e	532.4	530.3	2.1	
	[17,709]	[104,173]		0.17
f	532.4	530.3	2.2	
	[20,291]	[96,269]		0.18
g	532.3	530.3	2.2	
	[15,613]	[86,738]		0.18
h	532.4	530.2	2.1	
	[17,933]	[98,452]		0.18
i	532.4	530.3	2.1	
	[16,337]	[90,759]		0.18
j	532.4	530.3	2.1	
	[18,877]	[92,356]		0.2
k	532.4	530.3	2.2	
	[7529]	[68,448]		0.11

[a] Corrected binding energy (B.E.) in eV referenced to C 1*s* = 284.6 eV. Peak 1 is attributed to surface hydroxyl sp, while Peak 2 is due to rhodium and magnesium oxides.

[b] Peak areas in brackets.

[c] Full-width at half maximum (FWHM) of peak in eV. Both peaks were fitted with the same FWHM and Gaussian/Lorentian ratio.

[d] Sample treatments are described in Table 1.

TABLE 4

Atomic Concentration Ratios after Various CO/He Adsorption Procedures on Rh/MgO

Treatment[a]	Rh/Mg	Rh/O	Rh/C	Mg/O	Mg/C	O/C
a	0.08	0.04	0.05	0.50	0.63	1.26
b	0.06	0.07	0.08	1.17	1.33	1.14
c	0.08	0.08	0.05	1.00	0.63	0.63
d	0.10	0.08	0.05	0.80	0.50	0.63
e	0.08	0.08	0.06	1.00	0.75	0.75
f	0.03	0.03	0.06	1.00	2.00	2.00
g	0.03	0.03	0.07	1.00	2.33	2.33
h	0.03	0.03	0.06	1.00	3.33	2.50
i	0.06	0.08	0.08	.573	3.33	3.33
j	0.06	0.06	0.08	1.00	1.33	1.33
k	0.05	0.11	0.06	2.20	1.20	0.55

[a] Sample treatments are described in Table 1.

true in the case of Rh/TiO_2 (*6*) but not in the case of Rh/Al_2O_3 (*2*, *28*) catalysts. It is noted that hydrogen reduction at 623 K, applied before the CO/He treatment at 423 K, did not prevent oxidation of Rh_x^0 crystallites by CO at 423 K.

When the temperature of CO adsorption was increased to 573 K, the Rh (3*d*) doublet corresponding to Rh^{n+} species disappeared, indicating elimination of Rh^{n+} species after these CO/He treatments (Figs. 3a and 3b). At the same time, there was a decrease in the Rh/Mg area ratio (Table 4) compared to those at lower adsorption temperatures. These results suggest a reductive/agglomeration effect on the Rh^{n+} species induced by CO at 573 K (Scheme II). This effect has also been demonstrated to take place on other Rh systems (*2*, *4*, *29*). Infrared work on the present catalyst showed the absence of gem-dicarbonyl CO species following adsorption at 573 K (*15*). This result is consistent with XPS results given here.

The deposition of surface carbon by the Boudouard reaction

$$2\ CO \rightarrow CO_2 + C \qquad (2)$$

on the present catalyst was studied (*14*). It was found that $q_c = 0.007$ and 0.015 at $T = 523$ and 573 K, respectively, after 2 min in 10% CO/He. The increase in the amount of deposited carbon with temperature may also play some role in the oxidation of rhodium. Carbon deposition may inhibit the oxidation of Rh via hydroxyl groups as in Eq. (1) by either reducing the disruptive capabilities of CO on the Rh_x^0 crystallites (changing the bonding of CO with Rh_x^0) or by covering part of the MgO surface (reducing the active $-OH$ concentration). Evidence for a change in CO binding was presented by CO TPD experiments (*14*). The Mg/O and Mg/C ratios increase at higher reaction temperatures suggesting that carbon coverage of MgO is unlikely. The XPS data presented here suggest therefore that significantly larger carbon concentrations exist on these catalysts than in earlier studies (*14*). This may lead to reductive agglomeration due to carbon on the Rh particles.

The experiment of Fig. 4a with a fresh reduced catalyst sample clearly demonstrates that for 5 min time on CO/He stream at 573 K that no oxidation to Rh^{n+} occurs. This result may also suggest that the absence of Rh^{n+} species in the freshly reduced sample is not due to depletion of $-OH$

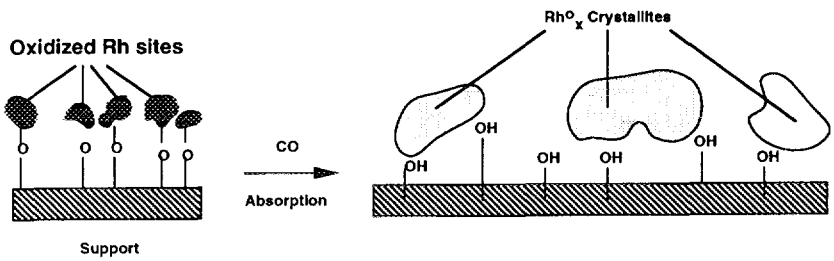

SCHEME II. Reductive agglomeration effect of CO absorption. CO/He treatments at temperatures greater than or equal to 573 K.

TABLE 5

Peak Area and Area Ratios of the Rh 3*d* (3/2) Region after Various Sample Treatments

Treatment[a]	B.E. (eV)	Area (units)	Area ratio of $Rh^{n+}/(Rh^{+} + Rh^{0})$
a	307.2	0	1.00
	310.7	71566	
b	307.2	191534	0.00
	309.2	0	
c	307.2	80534	0.47
	309.9	72132	
d	307.2	77228	0.43
	309.8	58952	
e	307.2	102020	0.46
	309.8	86891	
f	307.2	155124	0.00
	309.8	0	
g	307.2	148258	0.00
	309.8	0	
h	307.1	147700	0.00
	309.8	0	
i	307.1	159998	0.00
	309.8	0	
j	307.2	157770	0.00
	309.8	0	
k	307.2	72446	0.06
	309.8	4797	

[a] Sample treatments are described in Table 1.

groups by successive CO adsorption cycles or to agglomeration of Rh_x^0 particles.

(*C*) *Effects of H_2 Reduction Temperature*

The effects of H_2 reduction temperature on the oxidative disruptive process of CO is demonstrated by comparing the Rh 3*d* spectra of Fig. 2b (reduction at 623 K, CO/He treatment at 300 K) and Fig. 4b (reduction at 773 K, CO/He treatment at 300 K). The amount of Rh^{n+} species in the sample reduced at 773 K is substantially decreased, and as Table 5 shows, the $Rh^{n+}/(Rh^{0} + Rh^{n+})$ peak area ratio decreased from 0.47 to 0.06 as the reduction temperature increased from 623 to 773 K. In addition, Table 4 shows that the Rh/Mg ratio decreased from ~0.08 to 0.05 at the higher reduction temperature, suggesting that larger Rh aggregates are formed on the Rh support. These results suggest that the larger Rh particles formed after H_2 reduction at 773 K retarded the CO-assisted oxidation of Rh_x^0. This explanation was also proposed by others (*30*).

Table 4 shows that the decreases in the Rh/Mg atomic ratios for sample treatment c (reduction at 623 K) and sample treatment k (reduction at 773 K) were accompanied by an increase in the Rh/O atomic ratio (Table 4).

Furthermore, Table 3 shows that the surface hydroxyl-to-oxide ratio (Peak 1/Peak 2) decreases from 0.17 to 0.11 in going from treatment c to treatment k. Results of Tables 3 and 4 both suggest that higher reduction temperatures result in reductive agglomeration of the Rh particles, as well as removing surface hydroxyl species from the surface of the MgO support.

CONCLUSIONS

The present work provided evidence that oxidation of Rh^0 to Rh^{n+} by CO chemisorption in the range 300–523 K does occur on the Rh/MgO catalyst as was found for Rh/Al_2O_3 (*2–5*) and Rh/TiO_2 (*6*) catalysts. However, increasing the CO/He adsorption temperature to 573 K results in the complete elimination of any Rh^{n+} species. A reductive agglomeration process due to carbon deposits induced by CO is suggested to occur. The effect of hydrogen reduction temperature on the oxidation of Rh by CO is significant. Increasing the reduction temperature from 623 to 773 K caused a significant decrease in the extent of oxidation of the Rh surface by CO/He at 300 K. Larger Rh_x^0 crystallites produced by H_2 treatment at 773 K accompanied by partial dehydroxylation of the MgO surface may explain this low degree of oxidation of Rh by CO/He at 300 K.

ACKNOWLEDGMENTS

We thank the Department of Energy, Office of Basic Energy Sciences, Division of Chemical Sciences for support of this work. We also thank Dr. William S. Willis for helpful discussions.

REFERENCES

1. van't Blick, H. F. J., van Zon, J. B. A. D., Huizinga, T., Vis, J. C., Koningsberger, D. C., and Prins, R., *J. Phys. Chem.* **87,** 2264 (1983).
2. Solymosi, F., and Pasztor, M., *J. Phys. Chem.* **89,** 4783 (1985).
3. Solymosi, F., Pasztor, M., and Rakhely, G. J., *J. Catal.* **110,** 413 (1988).
4. Zaki, M. I., Kunzmann, G., Gates, B. G., and Knozinger, H., *J. Phys. Chem.* **91,** 1486 (1987).
5. Basu, P., Panaytor, D., and Yates, J. T., Jr., *J. Phys. Chem.* **91,** 3133 (1987).
6. Buchanan, D. A., Hernandez, M. E., Solymosi, F., and White, J. M., *J. Catal.* **125,** 456 (1990).
7. Solymosi, F., and Knozinger, H., *J. Chem. Soc. Faraday Trans.* **86**(2), 389 (1990).
8. Dai, G. H., and Worley, S. D., *J. Phys. Chem.* **90,** 4219 (1986).
9. Tan, B. J., Ph. D. thesis, Kansas State University, 1989.
10. Tan, B. J., Sherwood, P. M. A., and Klabunde, K. J., *Langmuir* **6,** 105 (1990).
11. Tan, B. J., Sherwood, P. M. A., and Klabunde, K. J., *Chem. Mater.* **2,** 186 (1990).
12. Tan, B. J., Sherwood, P. M. A., and Klabunde, K. J., *J. Am. Chem. Soc.* **113,** 855 (1991).
13. Hooker, P., Tan, B. J., Klabunde, K. J., and Suib, S. L., *Chem. Mat.* **3,** 947 (1991).
14. Efstathiou, A. M., *J. Mol. Catal.* **69,** 41 (1991).
15. Chafik, T., Efstathiou, A. M., and Bianchi, D., manuscript in preparation.
16. Efstathiou, A. M., Ph.D. thesis, University of Connecticut, 1989.
17. Daniach, S., and Sunjic, M., *J. Phys. C* **3,** 285 (1970).
18. Hufner, S. K., and Wertheim, G. K., *Phys. Rev. B* **11,** 678 (1975).
19. Wertheim, G. K., and Buchanan, D. N. E., *Phys. Rev. B* **16,** 2613 (1975).
20. Vegh, J., *Surf. Interface Anal.* **18,** 545 (1992).
21. Respoux, M., *Surf. Interface Anal.* **18,** 567 (1992).
22. (a) Sherwood, P. M. A., "Practical Surface Analysis" (D. Briggs and M. P. Seah, Eds.), 2nd ed. Chichester, West Sussex, England, Wiley, New York, 1990; (b) Proctor, A., and Sherwood, P. M. A., *Anal. Chem.* **54,** 13 (1982); (c) Tougaard, S., and Sigmund, P., *Phys. Rev. B* **25,** 4452 (1982); (d) Tougaard, S., *Surf. Interface Anal.* **11,** 453 (1988); (e) Tougaard, S., *Surf. Interface Anal.* **13,** 225 (1988).
23. (a) Gysling, H. J., Monnier, J. R., and Apai, G., *J. Catal.* **103,** 407 (1987); (b) Kuzniki, S. M., and Eyring, E. M., *J. Catal.* **65,** 227 (1980); (c) Lars, S., Anderson, T., and Scinell, M. S., *J. Catal.* **71,** 233 (1981); (d) Givens, K. E., and Dillard, J. G., *J. Catal.* **86,** 108 (1984).
24. Nacoache, C., Ben Taarit, Y., and Boudart, M., *Am. Chem. Soc. Symp. Ser.* **40,** 155 (1977).
25. (a) Wagner, C. D., Zatko, D. A., and Raymond, R. H., *Anal. Chem.* **52,** 1445 (1980); (b) Haycock, D. E., Nicholls, C. J., Urch, D. S., Webber, M. J., and Wiech, G., *J. Chem. Soc. Dalton Trans.*, 1785 (1978).
26. (a) Dharmadhikari, V. S., Sainkar, S. R., Badrinarayan, S., and Goswami, A., *J. Electron. Spectrosc. Relat. Phenom.* **25,** 181 (1982); (b) Nefedov, V. I., Gati, D., Dzhurinskii, B. F., Sergushin, N. P., and Salyn, Y. V., *Zh. Neorg. Khim.* **20,** 2307 (1975).
27. Goldfarb, D., Kevan, L., and Contarini, S., *J. Chem. Soc. Faraday Trans. 1* **84,** 2335 (1988).
28. Basu, P., Panayotor, D., and Yates, J. T., Jr., *J. Amer. Chem. Soc.* **110,** 2074 (1988).
29. Yates, D. J. C., Murrell, L. L., and Prestridge, E. B., *J. Catal.* **57,** 41 (1979).
30. Solymosi, F., and Pasztor, M., *J. Phys. Chem.* **90,** 5312 (1986).